SEISMIC REFRACTION INTERPRETATION WITH VELOCITY GRADIENT AND DEPTH OF INVESTIGATION

Michael L. Rucker
AMEC Earth & Environmental, Inc.
Phoenix, Arizona; michael.rucker@amec.com

Abstract

Traditional interpretation of seismic refraction data has used a concept of layered horizons or zones where each horizon has a discrete a seismic velocity. Software packages are now available that analyze and present seismic velocity as a continuously varying gradient across a grid or mesh. Such packages may utilize optimizing methods coupled with finite element or finite difference concepts to achieve interpretations. The resulting velocity gradient style of interpretation presents very different representations of the subsurface compared to traditional interpretations. These differences include advantages, disadvantages and conceptual challenges in utilizing the results. A profound advantage is an explicit interpretation of depth of investigation defined by the grids utilized in the interpretation. The author has observed that interpretations in geologic environments containing velocity reversals, where an underlying horizon seismic velocity is lower than in the overlying horizon, the velocity gradient method tends to interpret shallow depths of investigation consistent with bottom depths of the higher velocity horizons. In geologic environments with gradually increasing velocities with depth due to increased confining pressure, such as thick or deep cohesionless granular deposits, the velocity gradient interpretation can be more realistic than a forced multi-layered interpretation. Abrupt increases in the gradient velocity with depth inconsistent with confining pressure may be a reasonable indicator of cemented or cohesive materials rather than cohesionless materials. However, the velocity gradient concept tends not to model true abrupt changes, such as discrete soil-rock boundaries with large seismic velocity contrasts, as well as more traditional interpretations. An interface depth must be interpreted from change in the velocity gradient rather than as a distinct boundary utilizing Snell's Law. Furthermore, rippability criteria developed over the last 30 or more years predates velocity gradient interpretation methods; velocities obtained by these methods may not match with traditional velocity interpretations. The author is presently performing interpretations using a combination of both traditional and velocity gradient interpretation to utilize the advantages of both concepts.

Introduction

Subsurface geology is traditionally visualized as a layered media when results from seismic refraction surveys are applied to geotechnical engineering applications. Interpretation methods based on the refraction of the first portion of the seismic wave have been known for many years (Jakosky, 1940). The advent of hand-held calculators in the 1970's and personal computers by the 1980's, as well as the development of practical seismographs for civil engineering use, has made seismic refraction a practical geotechnical exploration tool for more than two decades. Recently, vastly increased computing power has now made computation-intensive software tools practical that can provide very different kinds of subsurface interpretation. These new software tools can help to address two basic questions of seismic refraction investigation. First, what is the depth of investigation of a seismic survey? Second, what alternative interpretations are available when the subsurface geology is not modeled well as a traditional layered media? Finally, interpretations incorporating velocity gradient can yield different results compared to traditional layered media interpretations. What are some of the implications of applying results from new interpretation concepts to long-term application experience learned using older, traditional interpretation concepts? For civil engineering applications, excavation rippability as a function of seismic velocity is perhaps the most critical of these issues that needs to be addressed. Among others, Redpath (1973) provides a general description of the seismic refraction method as applied to civil engineering, and Rucker (2000) describes applications of the method to highway and other transportation projects.

Interpretation Concepts

For purposes of this discussion, two primary interpretation methods are considered. Velocity gradient interpretation is represented by non-linear optimization (Optim, 2001), and traditional layered interpretation is represented by the intercept-time method (ITM). These interpretation concepts are detailed by Rucker (2000), and briefly reviewed here. Both methods provide seismic velocity, typically determined from the first arrival of the compression wave (p-wave), as part of the results of interpretation. Many other interpretation methods are available and are used by the geophysical profession. The physics of the seismic refraction method prevents straightforward detection and interpretation of lower velocity layers or zones underlying higher velocity layers. In this situation, the propagation of the refraction seismic energy at an interface between layers of different velocities occurs downwards rather than upwards, and the necessary assumptions for normal interpretation are violated.

Non-linear Optimization

The non-linear optimization interpretation includes gradational, gradual velocity changes and an explicit interpretation of travel paths for the first arrival seismic energy passing through the subsurface. A commercially available non-linear optimization routine (utilizing a simulated annealing routine) using a finite-difference model mesh to calculate travel times represents a recent advance in ray-tracing interpretation similar to tomography. An example interpretation of a 12-geophone array deployed on an embankment fill with shotpoints (where seismic energy is applied) at the array ends, center and quarterpoints, is presented in Figure 1. The software performs tens of thousands of iterations to obtain best matches between actual arrival times and distances between sources and receivers and modeled, calculated times based on ray paths through the finite-difference mesh. Each element of the finite-difference array is provided with a
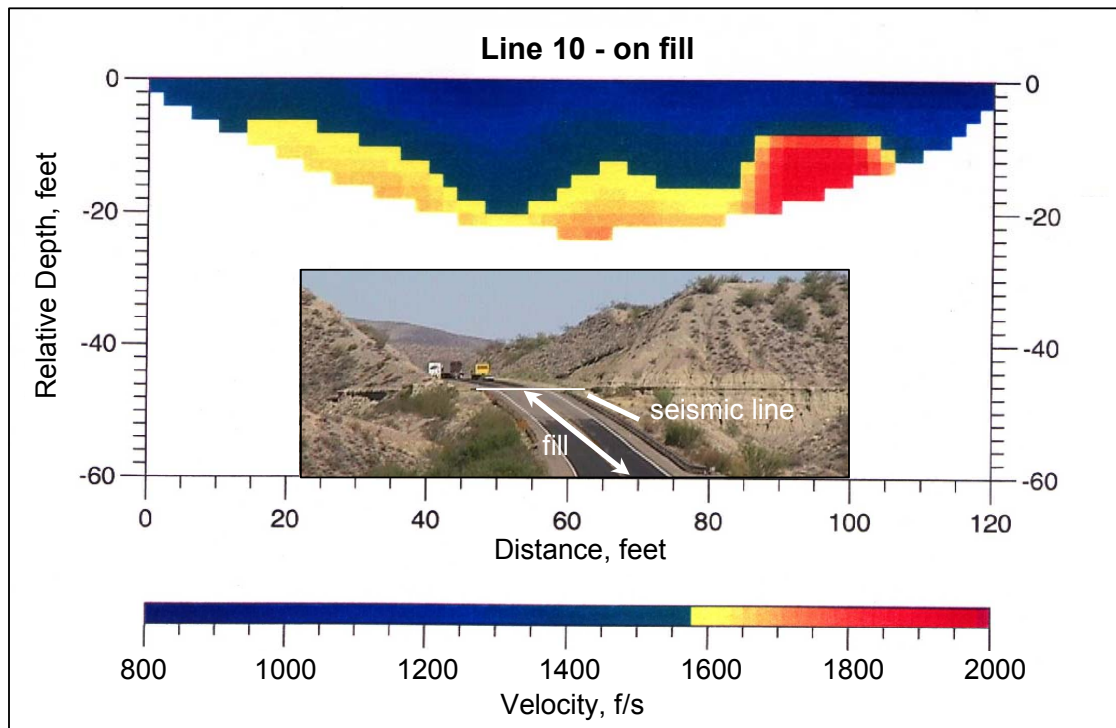

Figure 1. *Example seismic refraction interpretation using non-linear optimization software. Field data was acquired using a 12-channel seismograph with 10-foot geophone spacing. The seismic line was deployed on an engineered fill adjacent to a cut slope. Seismic wave velocities are in feet per second (f/s).*

Figure 2. *Example ITM interpretation with apparent depth of investigation from optimization interpretation. Upper photo shows exposed limestone at the proposed excavation cut. The center plot shows the ITM and depth of investigation interpretation. The lower plot shows the time-distance plots for the seismic first arrival data. Project units are metric, and seismic wave velocities are in meters per second (m/s).*
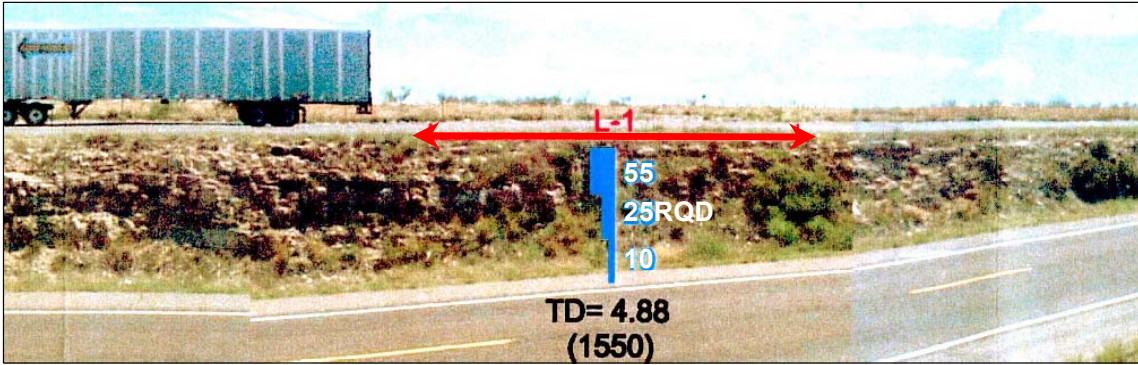
Subsurface Profile Interpretation of Refraction Seismic Data
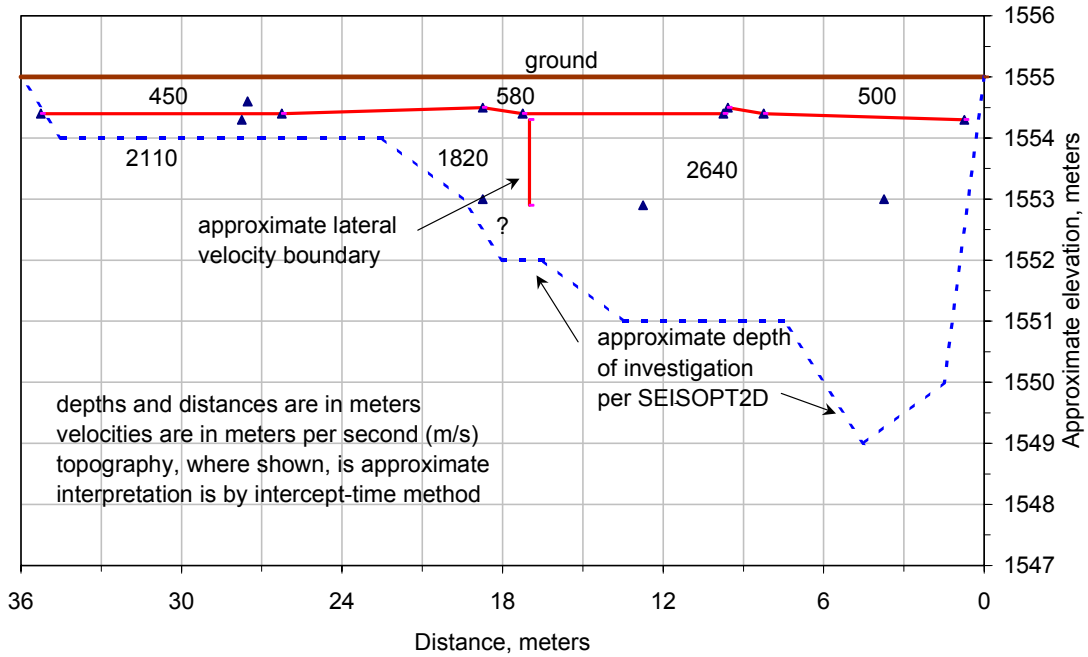
Time-Distance Plots (interpreted velocities & depths omitted for clarity)
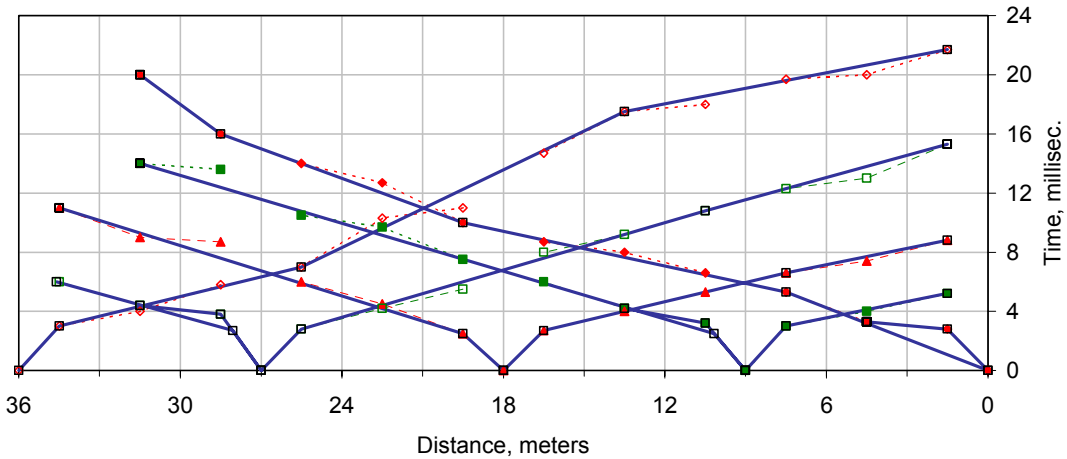
velocity through the optimized interpretation. Elements that are not parts of ray-paths do not have a velocity; the extent of the investigated zone is the part of the finite-difference mesh with optimized velocities. Results of interpretations are typically presented in color bar form, with different velocities presented as different colors. Interpretation results can also be converted into spreadsheet files of grid coordinates and velocities for further analysis.

Intercept-Time Method (ITM)

Interpretation by ITM assumes that the subsurface material layers or zones are present, and that each layer has a uniform velocity. Lateral changes in velocity, especially in shallow portions of the subsurface profile interpretation, are detected by interpreting data between adjacent shotpoints as smaller, shorter seismic lines. An example interpretation of a 12-geophone array deployed on a shallow limestone exposure, again with shotpoints at the array ends, center and quarterpoints, is presented in Figure 2. Velocities are interpreted by determining straight-line (or nearly straight-line) slopes along the various portions of a time-distance plot of the arrival of the first seismic signal at the various geophone locations. Velocities are calculated as distances traveled divided by time elapsed for each portion of the time-distance plot. A minimum of three data points are needed to confidently interpret each velocity slope. Thin layers whose influence is less than three data points cannot have velocities confidently interpreted, and typically may not be detected. Interfaces between different velocity material zones are assumed to be planar, although dipping interfaces can be readily interpreted. Depth interpretation formulas are used to calculate depths of interfaces between different velocity materials.

Depth of Investigation

Depth of investigation is a basic investigation parameter that is frequently misunderstood or not adequately addressed and quantified. This is especially true of engineers and managers who do not understand the geophysics but depend upon the results of the seismic refraction work. The very idea of depth of investigation can be separated into two concepts that are illustrated in Figure 3 utilizing concepts of ITM interpretation. One concept is that the depth of investigation is confined to the zone through which the seismic energy detected as first arrivals actually passes. The author will define this as an apparent depth of investigation. Another concept of the depth of investigation is that field parameters such as source strength and geophone array limit detecting refracted first arrival energy from deeper high velocity layers. Such layers might or might not be present within a relevant depth of interest. The author will define this as an implied depth of investigation.

As can be seen in Figure 3, the maximum depth of investigation is not uniform along a seismic line array. For a setup where the shotpoint is no farther than a short distance from the ends of the geophone arrays (no offset shots), the maximum depth of investigation will normally occur towards the center of the geophone array. It becomes shallower at locations closer to the energy sources. Thus, without offset shots, interpretation results that present seismic velocities and interface depths at depth beneath the shotpoints at the ends of an array are not based on seismic energy and ray paths that passed directly under or near those shotpoints at depth. Adjacent seismic lines can be partially overlaid in order to improve depth coverage at the ends of each line.

Apparent Depth of Investigation

Refraction of seismic energy occurs at boundaries between zones, layers or horizons of materials with differing seismic velocities. In order for the seismic energy refracting back towards the ground surface and the receiving geophone array to be the detected first arrival from a deeper layer, each layer velocity must increase with depth. Referring to Figure 3, the velocity V_1 in the uppermost subsurface layer must be less than the underlying second layer velocity V_2 to obtain interpretable refraction data and calculate the interface depth D_1. If V_2 is less than V_1, then the fastest travel time between the seismic source shotpoint to each of the geophones along the

entire geophone array will be through the shallowest layer, and no second layer velocity or interface depth can be interpreted. If V_2 is greater than V_1, then both velocities V_1 and V_2, and the interface depth D_1 can be interpreted. However, if there is not an additional higher velocity layer underlying the second layer within a depth sufficiently shallow to be detected by the geophone array, then no additional refraction seismic information is obtained below the depth D_1 interface between the two layers. The *apparent depth of investigation* that the interpreter can be confident of in this example is limited to the depth D_1. This is the zone through which the first arrivals of the seismic energy are represented by the data summarized in the time-distance plots.

In fact, using the Figure 3 example, several conditions could exist below the apparent depth of investigation. It is possible that the second layer with velocity V_2 could extend to a very great depth. The second layer could extend to the depth D_2 where an underlying higher velocity is present but not detectable because the receiving geophone array is not sufficiently long. Another possibility is that an underlying third layer is present, but has a velocity V_3 that is lower than V_2. This condition is known as a velocity reversal. Finally, there could be a gradual increase in velocity with depth at or below the second layer that results in a gradual change in the slope of the time-distance plot that cannot be effectively interpreted.
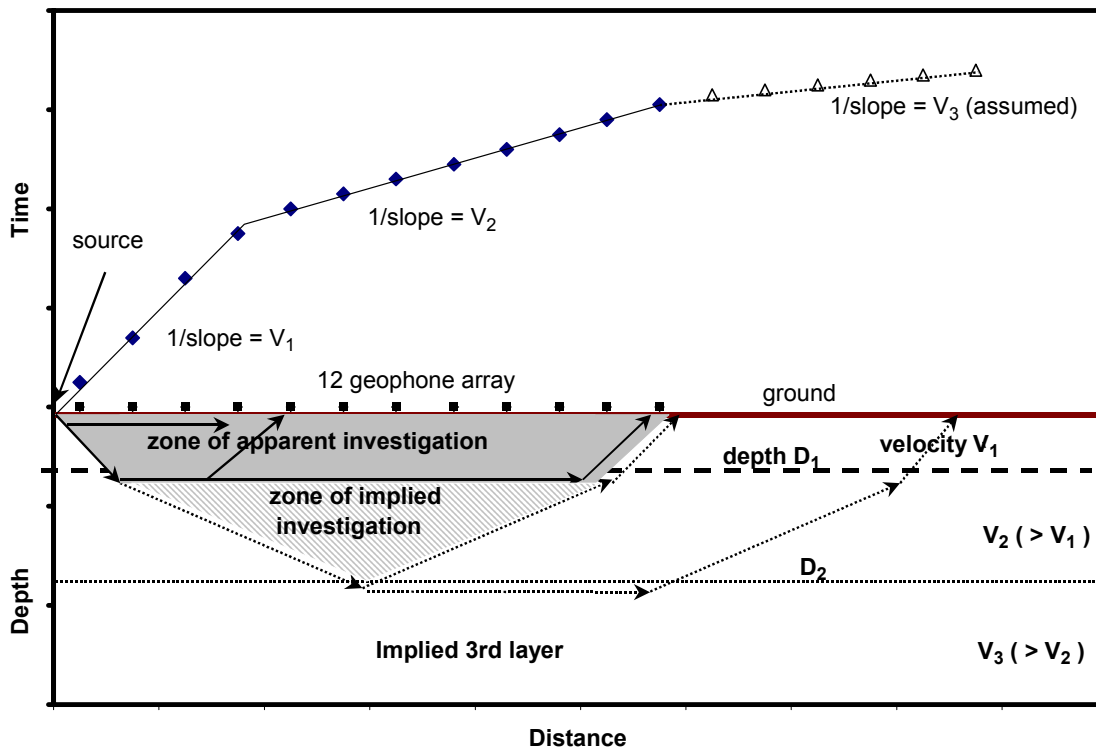

Figure 3. *Conceptual ITM interpretation of apparent and implied depths of investigation. A 12-geophone array with seismic energy source at the end is assumed. Only slopes V_1 and V_2 can be derived from the seismic waves detected by the geophone array. Velocities within each subsurface layer are assumed to be uniform.*

Implied Depth of Investigation

For the case where no velocity reversal is present, a minimum depth or thickness for the deepest interpreted layer, an *implied depth of investigation*, can be estimated. Figure 3 presents a procedure to make such an estimate. An imaginary, higher velocity segment is added to the time-distance plot beyond the limit of the actual data; in Figure 3 this is the V_3 portion of the plot. An imaginary deeper layer, the implied third layer in Figure 3, is thus added and an imaginary interface depth D_2 can be calculated. Of course, the calculated depth D_2 is dependent upon the

assumed velocity V_3, so that this implied depth of investigation is only an estimate. Due to Snell's Law, the angles of the propagating seismic wave front vary between layers to yield an implied depth of investigation that is limited to the center portion of the geophone array. This depth of investigation also becomes shallower towards the ends of the geophone array.

As a 'rule of thumb,' depths of investigation for refraction seismic lines (without far offset shots) are typically considered to be about one-quarter to one-third of the lengths of the lines. As this discussion illustrates, the actual portion of the depth of investigation represented by true seismic first arrival time data may be significantly less. Conditions within an implied zone of investigation may not be known with any confidence. A velocity reversal condition underlying the apparent zone of investigation may represent a very different subsurface ground condition from an interpretation of a seismic line based on implied depth of investigation. Furthermore, for both apparent and implied depths of investigation, the depth of investigation varies along the length of the seismic line. It is normally deepest towards the center and becomes shallower towards the ends.

Interpreting Depths of Investigation

Depths of investigation as well as seismic velocities can be effectively estimated as part of the interpretation and presentation process. As is true with the application of the seismic refraction technique, the presence of velocity reversals or other geologic conditions can limit the effectiveness of such estimates. Using traditional interpretations such at ITM, the deepest interpreted layer interfaces can be considered to be apparent depths of investigation. Using non-linear optimization, the limits of the finite-difference grids actively utilized in the optimized interpretation can be considered to be apparent depths of investigation. An advantage of using the non-linear optimization interpretation for depth of investigation is that an allowance for a gradual increase of seismic velocity with increasing depth is provided. Such an interpretation is presented in Figure 1, where an embankment fill exhibits a gradual velocity increase with depth that is consistent with an increase in modulus with increasing overburden or geostatic pressure. The maximum apparent depth of investigation is about 24 feet at the center of the 120-foot long array, and the zone of apparent interpretation is in the shape of a half ellipse. The equivalent ITM deepest interpretation (not shown) at Figure 1 is about 24 to 27 feet. In Figure 1, the apparent depth of investigation is nearly as deep as an anticipated implied depth of investigation. In contrast, Figure 4 presents an interpretation of another 120-foot long seismic line on a cemented soil cap overlying basin alluvial material. This interpretation exhibits a very shallow apparent depth of investigation of about 4 to 6 feet for about two-thirds of the seismic line length, and a maximum depth of investigation at the top of the highway cut of only 12 feet.

Experience using both interpretation methods together as a combined interpretation provides insight into possible complex subsurface conditions at a seismic line. Figure 2 provides an example of a complex subsurface profile in a limestone setting. Half of the line has an apparent depth of investigation of only 1 meter according to the optimization interpretation, and a material interface depth of about 0.5 to 0.7 meters according to the ITM interpretation. The other half of the line has a maximum apparent depth of investigation of about 6 meters according to the optimized interpretation, although ITM maximum interface depth of investigation interpretations are limited to depths of about 0.5 to 0.7 meters with a possible deeper interface at about 2 meters depth. The 'rule of thumb' anticipated implied depth of investigation for this 36-meter line might be about 9 to 12 meters. Without an explicit interpretation of the depth of investigation, material below this shallow apparent depth of investigation might be mischaracterized. With the explicit interpretation showing a shallow apparent depth of investigation, the underlying material is shown to not be included in the characterization based on seismic refraction results.

Another example showing significant differences in soil cementation in a much younger alluvial basin setting is presented in Figure 5. The photograph shows cementation, typically at depths of about 2 to 4 feet, at an arroyo wall at the site. Two nearby 60-foot lines, Line B with
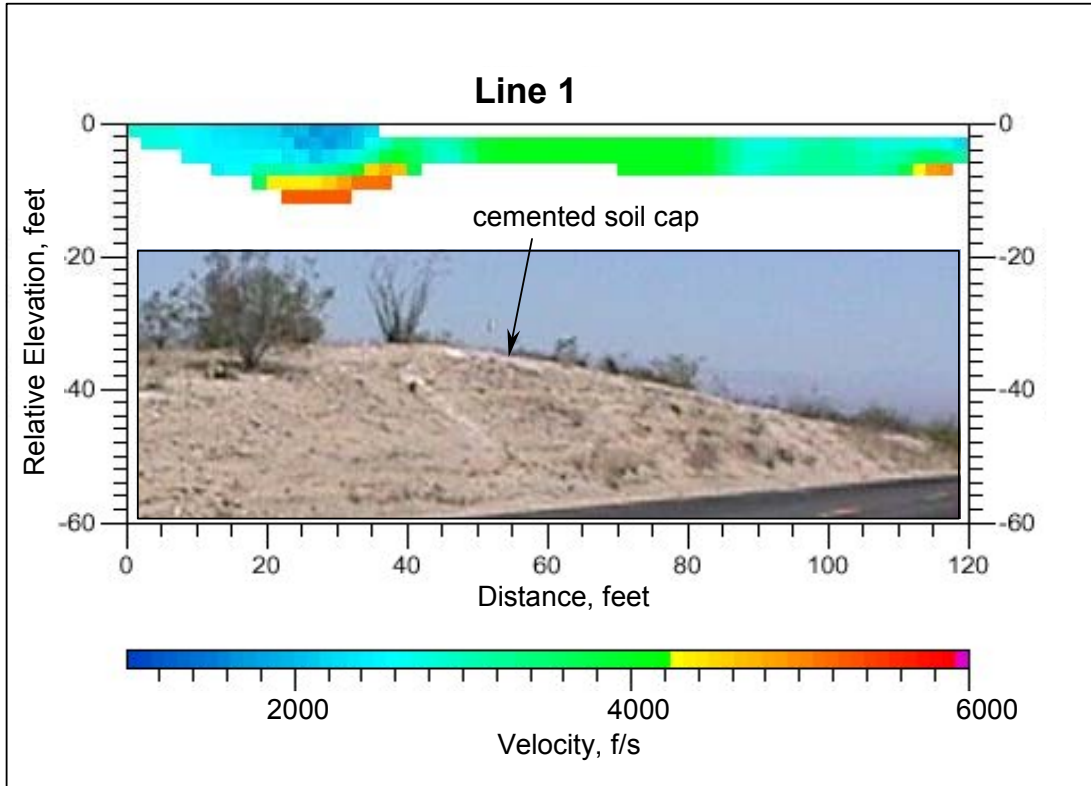
Line 1

cemented soil cap

Figure 4. *Example optimization interpretation showing very shallow depth of investigation due to a cemented soil cap overlying old basin alluvium deposits. The ITM interpretation (not shown) resulted in velocities of about 4,700 f/s beginning at depths of 1 to 4 feet.*

seismic velocities of 2,000 to 2,100 feet per second (f/s) beginning at depths of 1 to 4 feet, and Line A with seismic velocities of 1,600 to 1,800 f/s beginning at depths of 3 to 5 feet, have very different depths of investigation. Maximum anticipated implied depths of investigation are about 15 to 20 feet. Maximum apparent depths of investigation range from about 16 feet at Line A to only about 2 to 4 feet at Line B. These very different depths of investigation are consistent with very different cementation conditions at the two lines. A cementation horizon in the soils at the line with a shallow investigation depth is much more developed than at the line with a deep investigation depth. A velocity reversal condition beneath the developed cementation horizon is also probable.

Velocity Gradient Interpretation

ITM interpretations can effectively characterize horizontal velocity changes by interpreting between shotpoints when multiple shotpoints are used across an array, but are limited to interpreting a few layers or horizons vertically (Rucker, 2000). Optimized interpretations provide for the possibility of characterizing velocity gradients in the vertical and horizontal directions. Optimization software that the author uses generates ASCII compatible files of the finite-difference grid coordinates and the optimized velocity for each grid. These files can be imported to spreadsheets for straightforward manipulation and interpretation. An example vertical velocity gradient, through the center of the optimization interpretation presented in Figure 1, is presented in Figure 6. Upon inspection, it can be seen that, beneath the first few feet in depth, the velocity to depth relationship is relatively smooth throughout the depth of apparent investigation.

Seismic velocity in a geologic material is related to the low-strain dynamic modulus of the material. Soil modulus is influenced by density, confinement and cementation.   Thus, P-wave
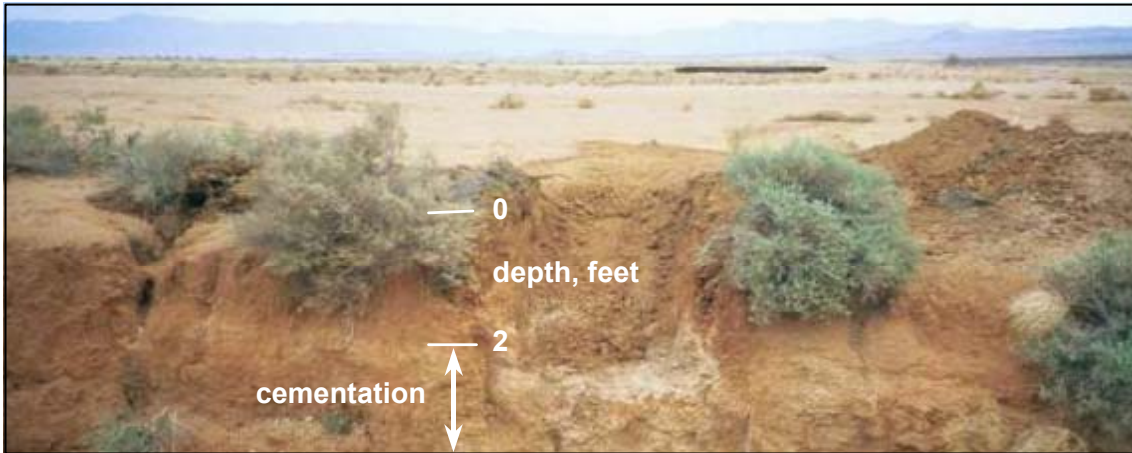
Line A Interpretation of Refraction Seismic Data
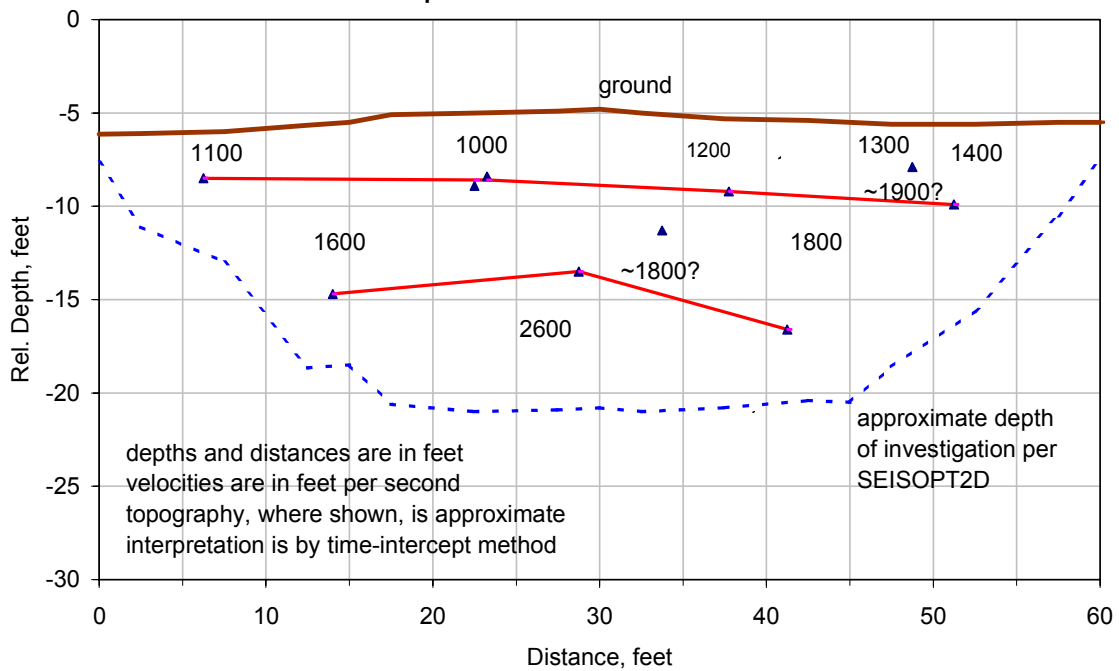
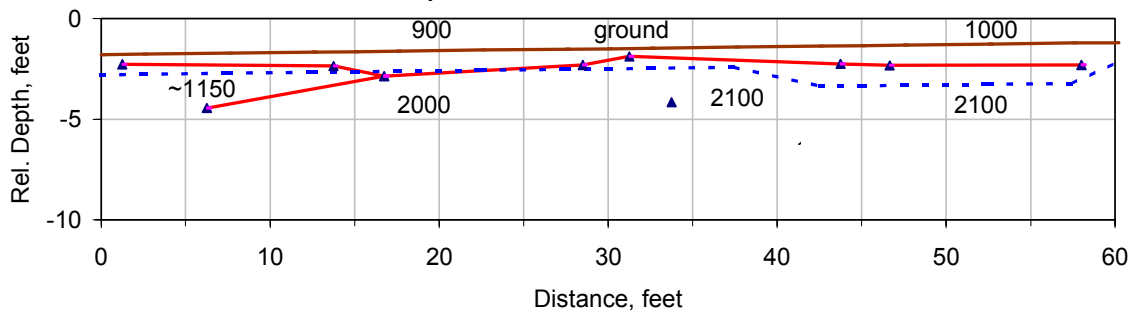**Line B Interpretation of Refraction Seismic Data**

Figure 5. *Example seismic lines in a variably cemented soil environment. Cementation at a depth of 2 to 4 feet is visible in the upper photo in an arroyo wall near Lines A and B. Line A indicates an area with relatively less cementation (lower velocities below depth of 2 feet) and a relatively deep apparent depth of investigation. Line B indicates an area with significant cementation (higher velocities) at a depth of about 2 feet and a very shallow apparent depth of investigation. Interpretation depth scales are relative to the project reference elevation.*

seismic velocity in a soil mass is influenced by density, confinement and cementation. Relationships between density, overburden pressure and modulus in cohesionless sands have been studied and refined since at least the 1960's. One of the older relationships (Richart *et al.*, 1970) that results in velocity change of cohesionless soil with depth, based on changes in soil modulus that scale to the square root of the effective stress at a given soil density, is presented in Figure 6. The interpreted vertical velocity gradient presented in Figure 6 matches very closely with that cohesionless soil relationship. Cohesionless material modulus manifested as seismic velocity is significantly controlled by the effective stress manifested as overburden pressure at subsurface depth.

Cementation provides material strength, and thus increased modulus, at least partly independent of overburden pressure and subsurface depth. At shallow depths with relatively little overburden pressure, cementation can result in higher seismic velocities than would occur without cementation. Seismic velocity at shallow depths can thus become an interpretation for the presence of cementation. Figure 7 presents vertical velocity gradients for the seismic lines presented in Figure 5 (actual optimization interpretations for Lines A and B are not presented). Line A in Figure 7 shows a gradually increasing velocity with depth similar to the cohesionless soil velocity-depth trend presented in Figure 6, although differences in soil densities result in different seismic velocities. There appears to be relatively little, if any, contribution by cementation to the seismic velocity in the shallow subsurface. Line B in Figure 7, however, has very little depth of investigation at all and a relatively high near surface velocity. This result is consistent with a significant contribution by cementation to the seismic velocity.
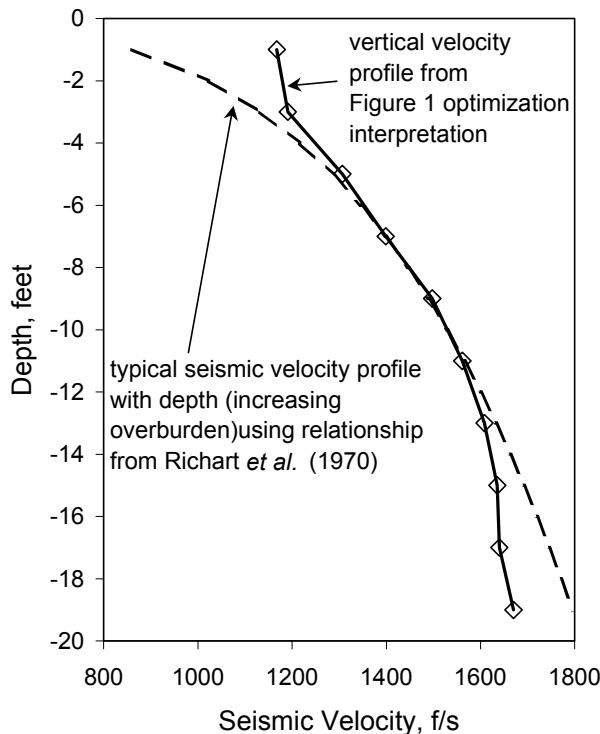

Figure 6. *Vertical velocity profile at midpoint of interpretation for highway fill section shown in Figure 1. Note the similarity to velocity-depth trend for cohesionless soils, where a density parameter in the Richart et al. (1970) relationship is varied until interpreted vertical velocity profile is matched.*
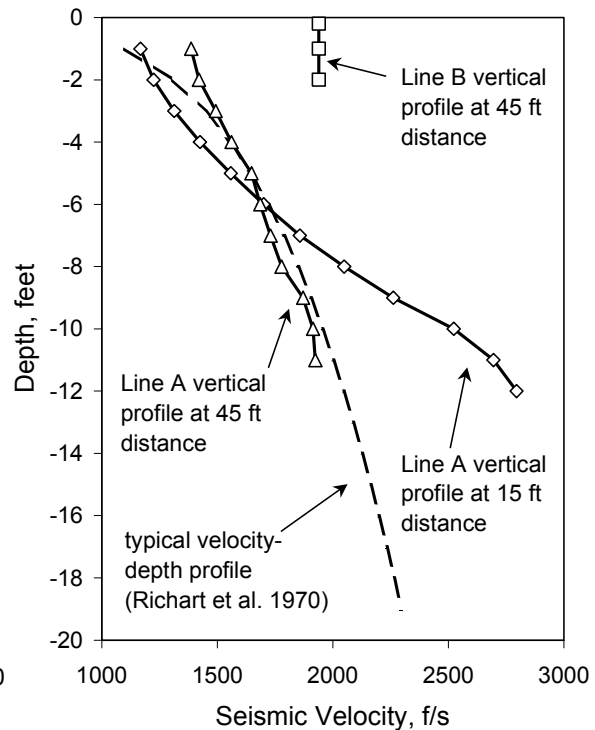
Figure 7. *Vertical velocity profiles from optimization interpretations (not presented) in cemented soil environment of Figure 5. Line B has velocities consistent with significant influence from cementation. Parameter in the Richart et al. (1970) relationship is varied until interpreted vertical velocity profile is matched.*

Seismic Velocity and Rippability

Charts that relate seismic velocities in various geologic materials to the ability of specific size and power bulldozers to excavate by ripping have been in existence almost since practical engineering seismographs first became available. The author has reviewed such charts back from the 1970's (Caterpillar, 1977). At that time, time-distance plots, ITM and similar interpretation methods that could be calculated by hand or graphical solutions were the only practical means to reduce data and obtain the necessary seismic velocities and interface depths. Rippability charts have not changed significantly over the years (Caterpillar, 1977, 1984, 1993, 2000), but rather have been revised to reflect changes in the bulldozer models. It is reasonable to assume that the seismic velocities presented in the current rippability charts are consistent with earlier velocities determined from these older interpretation methods. Thus, the author considers seismic velocities obtained from time-distance plots, with appropriate further analysis for dip, etc., to be the best representation of velocities to characterize rippability based on available charts. Differences in seismic velocities obtained using radically different interpretation methods such as non-linear optimization need to be examined to avoid misunderstandings and misapplications to the rippability charts used by the engineering and contracting professions.

The non-linear optimization software manuals familiar to this author explain about redefining subsurface layer interfaces from a velocity gradient interpretation. That issue does not need to be discussed here. At present, some software has limits of 250 percent on the maximum velocity change between finite-difference grid elements. The author works primarily in the arid southwest U.S. and commonly interprets soil-rock interfaces with a velocity contrast far greater than 250 percent. In wetter climates with relatively shallow water tables, velocity contrasts at the water table interface may similarly be quite large. Optimization software is forced to 'spread out' the interface over several grid elements or overestimate the lower velocity and underestimate the higher velocity to accommodate that contrast. It is important that the interpreter be able to discern when such situations arise and use appropriate judgment in the interpretations. Perhaps an effective rule is that when the optimization interpretation shows a very shallow depth of investigation, if reasonable seismic velocities are important, then they should be interpreted by other means.

An issue of concern about characterizing rippability, however, relates to the size of the finite-difference grids and resulting interpreted velocities in situations of shallow rock. Figure 2 presents such a situation (optimization interpretation velocities are not shown in the figure). Using a geophone array with 3-meter spacings, there is a practical limit of about 1-meter for each grid element size. Along the left half of the Figure 2 interpretation at about (36 to 18 meters distance), the optimization interpretation velocities for the grids are typically 1,300 to 1,800 m/s (4,300 to 5,900 f/s). However, velocities range from a low of 1,080 m/s (3,500 f/s) to a high of 2,680 m/s (8,800 f/s) at single cells in this area. These velocities are indicated as being present at the ground surface in the optimization interpretation. The ITM interpretation has a 450 m/s (1,500 f/s) soil layer to an interface depth of about 0.5 to 0.7 meters, with an underlying rock velocity of 2,100 m/s (6,900 f/s). Based on the ITM results, two materials with a velocity contrast of nearly 500 percent are forced into a single grid element in the optimization interpretation. The engineer is faced with having to select a representative velocity from a velocity range. It is likely that a selected velocity based on many of the grids would be around 1,800 m/s (5,900 f/s) or less, which is much lower than the 2,100 m/s (6,900 f/s) obtained from the ITM interpretation. An incorrect selection of ripping equipment could be made in this situation. Using a smaller geophone spacing in the field could permit reducing the finite-difference grid size to improve characterization of the soil/rock interface and velocities, but project coverage would be reduced and/or field data acquisition costs would rise.

Figure 4 presents another case where a shallow soil cover is present over a harder material. ITM interpretations are not presented in the figure. Ten-foot geophone spacings result in a practical finite-difference grid size of 2 feet. Over most of the line, optimization interpretation velocities are typically in the range of 3,000 to 4,000 f/s, and no surficial soil cover is interpreted.

The ITM interpretation has a 1,200 to 1,600 f/s soil layer to an interface depth of 1 to 3 feet, with an underlying cemented soil (caliche per rippability chart) layer velocity of 4,700 f/s. Again, the optimization interpretation appears to be underestimating seismic velocity when compared to the ITM interpretation, and an incorrect selection of ripping equipment could be made.

Summary

New software capabilities that perform interpretations as velocity gradients are improving the ability to include depths of investigation in seismic refraction interpretations. Identification of cohesionless versus cohesive soil deposits (above the water table) may be possible utilizing velocity gradients. Differences in interpretation methods and results may limit the applicability of velocity gradients in rippability studies and water table depth determination in some situations. The combination of interpreting both by non-linear optimization and traditional methods permits applying the strengths of each method and interpretation cross-checks, and permits explicit interpretation and presentation of reasonable depths of investigation for the results of each seismic line.

References

Caterpillar Tractor Company (Caterpillar), 1977, *Caterpillar Performance Handbook* 7th Edition, Peoria, Illinois.

Caterpillar Tractor Company (Caterpillar), 1984, *Caterpillar Performance Handbook* 15th Edition, Peoria, Illinois.

Caterpillar Tractor Company (Caterpillar), 1993, *Caterpillar Performance Handbook* 24th Edition, Peoria, Illinois.

Caterpillar Tractor Company (Caterpillar), 2000, *Caterpillar Performance Handbook* 31st Edition, Peoria, Illinois.

Jakosky, J.J., 1940. *Exploration Geophysics*, Trija Publishing Company, Los Angeles, California.

Optim, 2001. User's Manual SeisOpt^R@2D^{TM} Version 2.8, Optim LLC, UNR-MS 174, 1664 N. Virginia St., Reno, Nevada.

Redpath, B.B., 1973. ΑSeismic Refraction Exploration for Engineering Site Investigations.≅ Technical Report E-73-4, U.S. Army Engineer Waterways Experiment Station, Vicksburg, MS.

Richart, F.E., Hall, J.R. Jr. and Woods, R.D., 1970, *Vibrations of Soils and Foundations,* Prentice-Hall, Englewood Cliffs, New Jersey.

Rucker, M.L., 2000. Applying the Seismic Refraction Technique to Exploration for Transportation Facilities, in Geophysics 2000, The First International Conference on the Application of Geophysical Methodologies to Transportation Facilities and Infrastructure, St. Louis, Missouri, December 11-15, Paper 1-3.